Combination of a Besocke-type scanning tunneling microscope with a scanning electron microscope

A. Emundts, P. Coenen, G. Pirug, B. Voigtländer,[a] and H. P. Bonzel
Institut für Schichten und Grenzflächen (ISG 3), Forschungszentrum Jülich, 52425 Jülich, Germany

P. Wynblatt
Department of Materials Science and Engineering, Carnegie Mellon University, Pittsburgh, Pennsylvania 15213

(Received 25 April 2001; accepted for publication 14 June 2001)

The article describes the combination of a Besocke-type scanning tunneling microscope (STM) with a scanning electron microscope (SEM) in an ultrahigh vacuum (UHV) environment. The open design of the Besocke STM allows the SEM to be implemented as an add-on of a high resolution electron column and a secondary electron detector. The combined instrument is capable of atomic resolution imaging by STM and real time SEM imaging. SEM resolution down to about 80 nm was achieved. Simultaneous operation of STM and SEM is possible. The operation and performance of the combined instrument is illustrated by a variety of examples. Although the instrument is suitable for a wide range of applications where a combination of atomic resolution with lower magnification imaging is required, its operation in an UHV environment makes it particularly appropriate for the study of reactive metal surfaces. © *2001 American Institute of Physics.*
[DOI: 10.1063/1.1392341]

I. INTRODUCTION

Instruments which combine capabilities of a scanning tunneling microscope (STM) and a scanning electron microscope (SEM) have been constructed previously by several different research groups. Two different approaches have been taken. Commercial SEM systems have been adapted to incorporate a STM stage[1–10] or STM systems have been retrofitted with a high resolution electron column to gain the additional benefit of SEM.[11–19] The latter systems operate mostly under true ultrahigh vacuum conditions ($<1\times10^{-10}$ mbar) and are particularly suitable for a wide range of surface science investigations. The need for instruments that allow imaging over a broader range of resolution than is available in STM was stated by Binnig and Rohrer in one of their first articles describing that technique:[11] ''For many applications, the STM is best used in combination with another microscope. An inherent limitation of STM is that it always operates at high resolution.'' However, beyond the need for a greater range of magnification, the availability of combined SEM and STM in a given instrument provides several additional advantages.

(a) The low magnifications available in the SEM allow observation of the approach of a STM tip towards a sample surface, thus providing more control and preventing tip crashes. This is particularly important for samples with surfaces which may be nonplanar, with localized height variations of several hundred nanometers, such as the ones that have been of particular interest in some of our own studies described in more detail below.

(b) With the availability of a fast scanning SEM, it also becomes far simpler to identify areas of potential interest for high resolution study, which might otherwise demand much wasted effort if only high resolution scans were available.

(c) A related issue is the relocation (or tracking) of a given area of interest for study by STM after (or during) one or more intervening treatments (e.g., annealing). Such treatments may require removal of a sample from the STM sample holder for processing in a preparation chamber, and its subsequent return for reexamination, upon completion of the treatment. Without some low magnification capability, it would be impossible or at least very time consuming to relocate a region investigated previously at high resolution.

(d) The STM tip itself can be readily imaged by the SEM. This capability is useful for examining the tip shape so as to assess its sharpness and its opening angle, or to detect evidence of tip crashes which may degrade STM image quality and require tip replacement.

(e) The availability of a SEM can also be useful for locating exactly dimensioned features on patterned substrates used for calibrating the lateral (x,y) magnification of STM images.

The article describes the combination of a Besocke-type (''beetle'') STM[20–22] with a SEM in an ultrahigh vacuum (UHV) environment. The operation of the instrument under UHV conditions is particularly suitable for the study of reactive surfaces, such as those of metals. To our knowledge this is the first attempt at adding SEM capabilities to this particular type of STM, and is of interest, given the special geometrical and other design constraints which are inherent in STMs of different types. One particular advantage of the Besocke-type STM is its open design which allows positioning of the SEM column within focusing distance to the

[a]Author to whom correspondence should be addressed; electronic mail: b.voigtlaender@fz-juelich.de

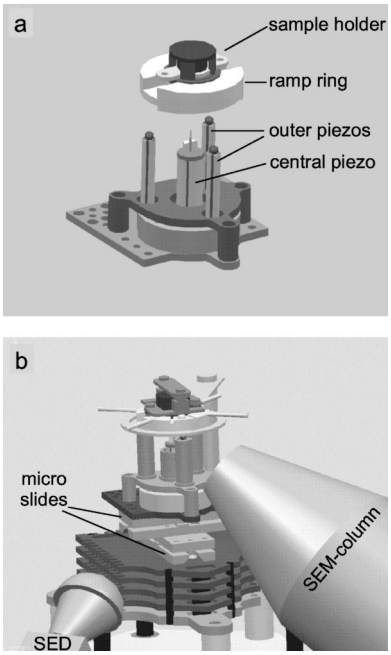

FIG. 1. (a) STM of the Beetle-type. (b) Detailed view of STM, SEM column, and secondary electron detector (SED).

sample, without undue interference from its various structural elements.

Our purpose in developing this instrument was to facilitate the study of the equilibrium crystal shape (ECS) of metals by STM.[23–27] This application requires measurement of the detailed three-dimensional shape of metal crystallites residing on a flat substrate made of a different material. A typical crystal, characterized by a contact angle at the crystal/substrate interface of 40°–60°, may be of the order of 1 μm in diameter and protrude a few hundred nanometers above the flat substrate. Whereas atomic resolution in the $(x\text{-}y)$ plane of the image is not essential, the imaging of monoatomic steps on the crystal surface is crucial. These particular performance requirements have influenced the characteristics of the STM component of the combined instrument.

II. INSTRUMENT CONFIGURATION

A. STM

The Besocke-type STM and criteria used in its design have been described in detail before.[20–22] Here we give only a brief description. A general view of the STM is displayed in Fig. 1(a). Sample and holder are supported by a cylindrical ramp ring which itself sits on three outer piezo-tube elements. The underside of the ramp ring is divided into three inclined sections to allow for vertical motion of the sample relative to the STM tip. By bending the three piezos appropriately, it is possible to translate the sample in any given direction, or rotate it.[20] The rotation on the ramp is used to move the sample in the z direction towards or away from the tip (coarse approach). The final z approach is accomplished by a fourth central piezo-tube scanner which carries the imaging tip. The tip is moved towards the sample until an electron tunneling current can be measured. Imaging of the surface is then achieved with the central piezo and tip which is to be rastered across the sample surface under tunneling conditions.

In the present instrument, the outer piezo drives are 12.8 mm long, whereas the center piezo scanner with the imaging tip is 19.1 mm long. This longer piezo scanner allows imaging of larger areas, and lends itself well to the observation of surface features of relatively large heights, such as the crystallites of interest. With this arrangement, the central piezo scanner with tip has a maximum dynamic range of about 10 μm in the z direction, and of 30 μm in the x and y directions. However, large area STM scans are generally avoided because of relaxation, long time creep, and nonlinear response of the piezo material,[28,29] all of which may cause undesirable image distortion. Furthermore, the total time to acquire a large scale image can be greater than 1 h, especially for rough surfaces or objects with a high aspect ratio. Because of these long times, thermal drift becomes a problem and is another source of image distortion. Hence large area, long time STM scans are impractical when high structural accuracy is required.

The whole STM assembly rests on two piezo-driven micropositioning slides (MS 5, Omicron), as shown in Fig. 1(b). These are used for larger translations of the STM assembly (up to a maximum of 5 mm, in steps of 40 nm), as further explained below. One of the principal problems of achieving high resolution in STM is the elimination of vibrations which may cause relative motions between the imaging tip and the sample. In the standard Besocke design, the piezo-drive assembly is vibrationally isolated from the surroundings by both springs (with low vibration transmission except close to some resonant frequency) and motion dampers consisting of a stack of Viton supports. This design had to be modified in combination with the added SEM imaging capability.

B. SEM

The SEM consists of an electrostatic two lens electron column with a Schottky emitter and electrostatic focusing optics (FEI Company). The emitter consists of a zirconium oxide coated tungsten filament operating at 1800 K and

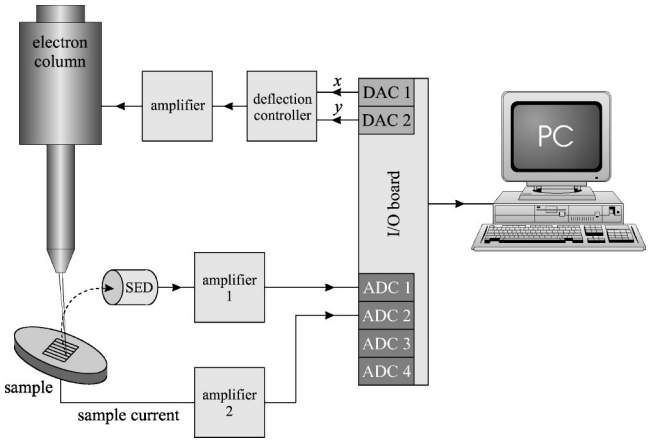

FIG. 2. Schematic of the SEM system; DAC: digital-to-analog converter, ADC: analog-to-digital converter, SED: secondary electron detector.

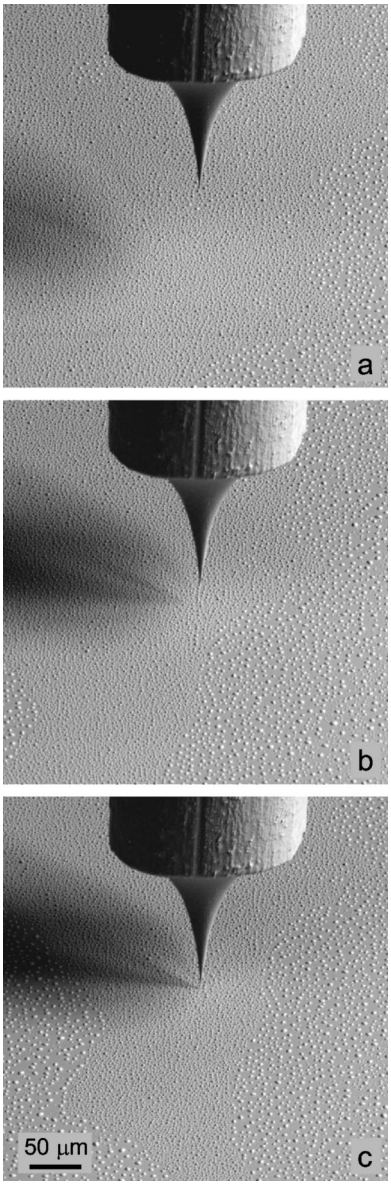

FIG. 3. Tip approach under STM control: (a) Large tip–sample distance, diffuse shadow; (b) approach of tip and sample results in a sharper shape of the shadow and a smaller distance between shadow and tip; (c) tip and sample are in tunneling contact, tip and shadow touch each other.

yielding a typical probe current of 1 nA.[30] The accelerating voltage is adjustable from 1 to 25 keV; however, all the work reported here was obtained using the maximum operating voltage. The optics of the SEM have been designed to allow a working distance of 20–25 mm between the nose of the SEM column and the sample. This large working distance is needed in order to avoid any mechanical interference between the various moving components of the STM and the SEM column. Nominal resolution of the column is 20 nm and the maximum raster size is about 2×2 mm.

A schematic block diagram of the SEM is shown in Fig. 2. Note that the sample normal does not coincide with the SEM column axis. For this reason, the large depth of focus typical of SEMs is particularly beneficial in the present combined instrument. Central to the SEM control and data analysis systems is an input/output card (PCI-MIO-16E-1, National Instruments) which provides two 16-bit digital-to-analog converters (DACs) for beam deflection and several 16-bit analog-to-digital-converters (ADCs) for processing of the image signals originating from either the secondary electron detector (SED) or the sample (in the case of absorbed current images). The software for operating this control system was provided by the Electronics Institute of the University of Wuppertal.[31,32]

The SEM column is differentially pumped by means of an added ion pump which is needed to maintain the required low pressure in the column. Furthermore, the column contains narrow passages which make it impractical to rely on the main chamber pumps. With this arrangement, the column pressure is typically one order of magnitude higher than that of the main UHV chamber. There is a column isolation valve which allows the main chamber to be brought up to atmospheric pressure without having to turn off the SEM filament or to replace the SEM filament without having to vent the main UHV chamber.

C. Combined system

The instrument consists of two main UHV chambers, a preparation chamber and an analysis chamber, connected by a gate valve. The preparation chamber includes facilities for sample heating or cooling, a physical vapor deposition system for the preparation of thin films of the crystallite material onto a substrate, and an ion gun for sputtering. The analysis chamber comprises the two microscopes and an Auger cylindrical mirror analyzer with a built-in electron gun to monitor the surface composition and cleanliness of the sample. The base pressure in both the preparation and main chambers is 7×10^{-11} mbar.

One of the principal technical problems that must be addressed in such an instrument is the relative vibrational motion between the sample on the STM stage and the tip, on the one hand, and between the sample/tip assembly and the SEM column, on the other. In order to avoid relative motions between the STM head and the SEM column, the vibration isolation springs of the Besocke design had to be eliminated. Instead, the sample holder was more tightly clamped to the STM stage by using a magnetic ramp and small permanent magnets located at the bottom side of the sample holder and below the bearing balls which terminate the three outer piezo-drives.[33] This has the effect of stabilizing the sample/tip configuration and at the same time the STM stage relative to the whole vacuum system and hence to the SEM column. On the other hand, vibrational motion of the SEM column, which is mounted on a flange of the UHV chamber, can occur relative to the STM stage. The amplitude of this vibration limits the achievable SEM resolution and its effect can be seen on highly magnified images of high contrast objects. This relative vibrational motion has been damped in the present instrument by a woven nylon strap which binds the external part of the SEM column to the main chamber. The success of this approach can be evaluated from the quality of the SEM images presented in the next section. The resolution achieved is about 80 nm instead of the nominal 20 nm.

A second important requirement for the combined use of STM and SEM is the capability to move the STM stage

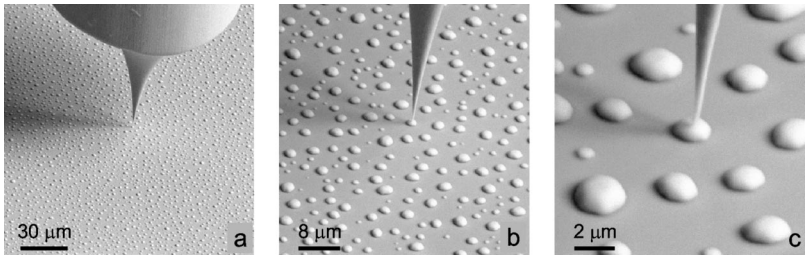

FIG. 4. SEM images of a Ru(0001) sample covered with Pb crystallites taken at different magnifications.

relative to the SEM column axis. This relative x,y motion ensures that the STM imaging tip can be positioned in the SEM optical axis, even at the highest magnification of the SEM. For this purpose there are the x- and y-piezo-driven microslides, Fig. 1(b), which support the whole STM stage (including sample) and allow its translation in x and y directions. Once the tip is in the SEM field of view, the SEM can be used to monitor the coarse and final approach of the sample to the tip and the selection of the sample area to be analyzed with STM.

III. INSTRUMENT OPERATION AND PERFORMANCE

In this section we will present several application examples for the combined use of SEM and STM. In this context it is also convenient to refer to our studies of equilibrium crystal shapes (ECS) to illustrate instrument operation and performance. In principle, the instrument is applicable to any purpose where the advantages of a combined STM-SEM would be beneficial, such as outlined in the Introduction.

Our first experimental example consists of three-dimensional Pb crystallites supported on a single crystalline Ru(0001) substrate. The size of the crystallites typically ranges from a few hundred nanometers to a few micrometers. A sequence of SEM images obtained during a STM tip approach to a typical sample surface is shown in Fig. 3. The distance between the tunneling tip and the surface can be estimated from the relative positions of the tip and of the shadow it casts on the sample surface. This shadow in the SEM image represents a region of weaker secondary electron detection from those parts of the sample surface which are partially blocked by the STM tip. In other words, when the tip is in the line-of-sight between the momentary point of secondary electron emission and the detector, the current recorded from that point is reduced. The tip shadow is essential for the evaluation of the distance between tip and sample. In Fig. 3(a), such a diffuse shadow of the tip may be seen on the left of the image. As the tip gets progressively closer to the surface, Figs. 3(b) and 3(c), the separation between the tip and its shadow gradually decreases. In fact, in Fig. 3(c) the tip and the sample are in tunneling contact. These images were acquired prior to adding the small magnets to the STM stage for improved stability. With the magnets present a multiple shadow appeared, presumably due to the local magnetic field.

Figure 4 shows a sequence of SEM images at different magnifications, taken with the STM tip in tunneling contact with the sample. Simultaneous SEM and STM operation is possible provided the tunneling current is chosen above a certain limiting value (in our case 0.3 nA). Another demonstration of imaging during an STM measurement is provided in Fig. 5, which shows a sequence of several SEM images acquired during operation of the STM.

The resolution of the STM part of the instrument is illustrated by the atomically resolved image of the reconstructed (7×7)-Si(111) surface of a flat Si crystal, shown in Fig. 6. Although atomic resolution in the plane of the sample is not crucial to many applications of this instrument, this figure demonstrates that high resolution is possible.

Figures 7(a) and 7(b) provide a comparison of SEM and STM images of the same object. The sample consists of a metal-coated glass slide with a regular array of circular depressions, about 1 μm in depth and a center-to-center distance of 1.5 μm, produced in the metallic overlayer. Images such as Fig. 7 are used for magnification calibration of the STM. The highest magnification image in this set [Fig. 7(c)] is taken close to the limit of resolution of the SEM. The edges of the holes are poorly resolved in the image, and from the length of the dark streaks at the edge one can estimate the effective SEM resolution to be about 80 nm. A higher rigidity of the chamber-flange connection is expected to eliminate

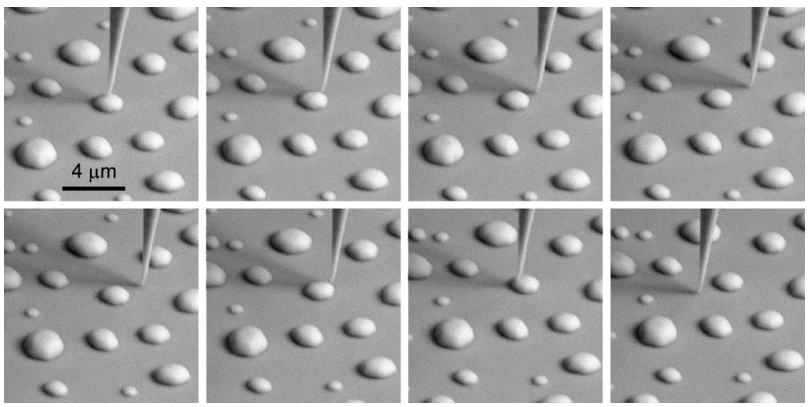

FIG. 5. SEM during a STM measurement (see also http://www.fz-juelich.de/video/emundts).

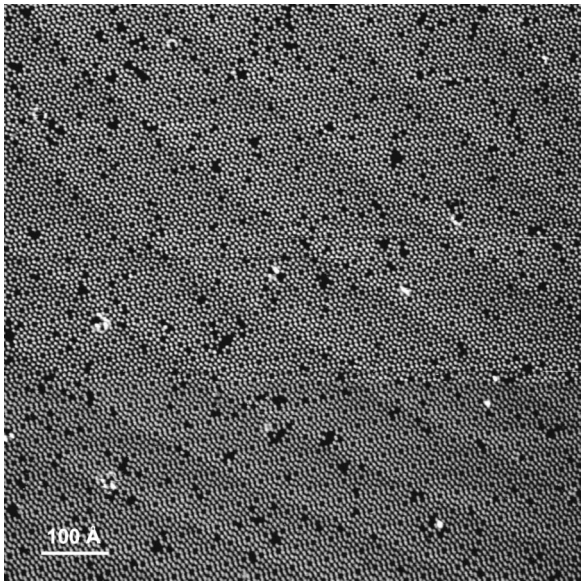

FIG. 6. Atomically resolved Si(111)-(7×7) surface.

the low-amplitude vibrations of the SEM relative to the STM stage and thus enhance the resolution.

Finally, we display in Fig. 8 a STM image of a single Pb crystallite, showing at the top a (111) facet. Although the atomic structure of the Pb(111) surface is not resolved in this case, the resolution of monoatomic steps near the edge of the facet is possible[24] and provides a precise determination of the outline of the facet. This localization of the facet edge, coupled with high precision measurement of the profile of the crystallite with increasing distance from the edge in various azimuthal directions, have allowed more detailed information to be obtained on the ECS of Pb than had previously been possible.[23–27] The combination of a Besocke-type STM and SEM column into a single instrument operating under UHV conditions makes it possible to study samples with significant surface roughness on the micrometer scale, without incurring STM tip crashes. In addition, no significant interference of one technique on the other has been noted. The instrument has been used with significant success to study the three-dimensional ECS of Pb crystallites, about 1 μm in size, on a flat Ru(0001) crystal, prepared in the same UHV system.

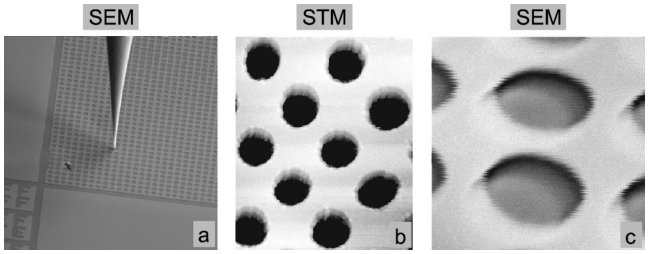

FIG. 7. (a) SEM image, (b) STM image, and (c) large magnification SEM image of a metal-coated glass slide used for magnification calibration. The circular depressions are about 1 μm in depth and have a center-to-center distance of 1.5 μm.

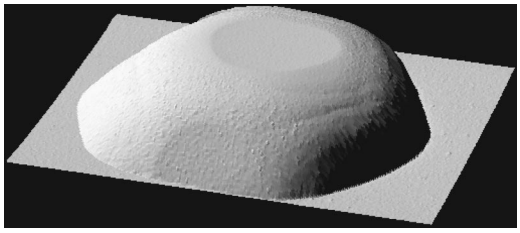

FIG. 8. Pb crystallite on a Ru(0001) substrate. Image size: 2.4×1.6 μm^2.

ACKNOWLEDGMENTS

The authors would like to acknowledge valuable discussions with U. Memmert in the early stages of the design of the STM/SEM combination. The authors acknowledge with thanks the Electronics Institute of the University of Wuppertal for providing the software used in the operation of the SEM. In addition, P. W. wishes to acknowledge support of several visits to the Forschungszentrum Jülich by the Alexander von Humboldt Foundation, and continuing support of his research in this area by the National Science Foundation under Grant No. DMR9820169.

[1] T. Ichinokawa, Y. Mayazaki, and Y. Koga, Ultramicroscopy **23**, 115 (1987).
[2] M. Anders, M. Mück, and C. Heiden, Ultramicroscopy **25**, 123 (1988).
[3] H. Fuchs and R. Laschinski, Scanning **12**, 126 (1990).
[4] A. O. Golubok and V. A. Timofeev, Ultramicroscopy **42–44**, 1558 (1992).
[5] A. V. Ermakov and E. L. Garfunkel, Rev. Sci. Instrum. **65**, 2853 (1994).
[6] R. J. N. Coope, T. Tiedje, S. L. Konsek, and T. P. Pearsall, Ultramicroscopy **68**, 257 (1997).
[7] A. Asenjo, J. Gómez-Herrero, and A. M. Baró, J. Microsc. **188**, 243 (1997).
[8] K. Nakamoto and K. Uozumi, Ultramicroscopy **42–44**, 1569 (1992).
[9] P. M. Thibado, Y. Liang, and D. A. Bonnell, Rev. Sci. Instrum. **65**, 3199 (1994).
[10] M. Troyon, H. N. Lei, and A. Bourhettar, Ultramicroscopy **42–44**, 1564 (1992).
[11] C. Gerber, G. Binnig, H. Fuchs, O. Marti, and H. Rohrer, Rev. Sci. Instrum. **57**, 221 (1986).
[12] G. C. Rosolen and M. E. Welland, Rev. Sci. Instrum. **63**, 4041 (1992).
[13] U. Memmert, U. Hodel, and U. Hartmann, Rev. Sci. Instrum. **67**, 2269 (1996).
[14] A. Wiessner, J. Kirschner, G. Schäfer, and T. Berghaus, Rev. Sci. Instrum. **68**, 3790 (1997).
[15] S. Maruno, H. Nakahara, S. Fujita, H. Watanabe, Y. Kusumi, and M. Ichikawa, Rev. Sci. Instrum. **68**, 116 (1997).
[16] Y. Naitoh, K. Takayanagi, H. Hirayama, and Y. Ohsima, Surf. Sci. **433–435**, 627 (1999).
[17] M. Takai, N. Yokoi, R. Mimura, H. Sawaragi, and R. Aihara, *Atomic-Scale Imaging of Surfaces and Interfaces Symposium*, edited by D. K. Biegelsen, D. J. Smith, and S. Y. Tong (Materials Research Society, Pittsburgh, 1993), pp. 23–28.
[18] Y. Naitoh, K. Takayanagi, Y. Oshima, and H. Hirayama, J. Electron Microsc. **49**, 211 (2000).
[19] A. Asenjo, A. Buendia, J. M. Gomez-Rodriguez, and A. M. Baro, J. Vac. Sci. Technol. B **12**, 1658 (1994).
[20] K. Besocke, Surf. Sci. **181**, 145 (1987).
[21] T. Michely and K. Besocke, J. Microsc. **152**, 77 (1988).
[22] J. Frohn, J. F. Wolf, K. H. Besocke, and M. Teske, Rev. Sci. Instrum. **60**, 1200 (1989).
[23] S. Surnev, P. Coenen, B. Voigtländer, H. P. Bonzel, and P. Wynblatt, Phys. Rev. B **56**, 12131 (1997).
[24] S. Surnev, K. Arenhold, P. Coenen, B. Voigtländer, H. P. Bonzel, and P. Wynblatt, J. Vac. Sci. Technol. A **16**, 1059 (1998).
[25] K. Arenhold, S. Surnev, P. Coenen, H. P. Bonzel, and P. Wynblatt, Surf. Sci. **417**, L1160 (1998).
[26] K. Arenhold, S. Surnev, H. P. Bonzel, and P. Wynblatt, Surf. Sci. **424**, 271 (1999).

[27] H. P. Bonzel and A. Emundts, Phys. Rev. Lett. **84**, 5804 (2000).
[28] R. W. Basedow and T. D. Cocks, J. Phys. E **13**, 840 (1980).
[29] K. R. Koops, P. M. L. O. Scholte, and W. L. de Koning, Appl. Phys. A: Mater. Sci. Process. **68**, 691 (1999).
[30] D. W. Tuggle and L. W. Swanson, J. Vac. Sci. Technol. B **3**, 220 (1985).
[31] P. Lepidis, I. Joachimsthaler, and L. J. Balk, Scanning **21**, 84 (1999).
[32] I. Joachimsthaler, Entwurf eines universellen Ansteuer- und Messsystems für Rastermikroskope. Bergische Universität GH Wuppertal, 1997.
[33] T. Michely, M. Kaiser, and M. J. Rost, Rev. Sci. Instrum. **71**, 4461 (2000).